Resonance Energy Transfer in a Calcium Concentration-Dependent Cameleon Protein

Satoshi Habuchi,* Mircea Cotlet,* Johan Hofkens,* Gunter Dirix,† Jan Michiels,† Jos Vanderleyden,† Vinod Subramaniam,§ and Frans C. De Schryver*

*Department of Chemistry, Katholieke Universiteit Leuven, Celestijnenlaan 200F, 3001 Heverlee, Belgium; †Center of Microbial and Plant Genetics, Kasteelpark Arenberg 20, 3001 Heverlee, Belgium; §Department of Molecular Biology, Max Plank Institute for Biophysical Chemistry, 37070 Göttingen, Germany

ABSTRACT We report investigations of resonance energy transfer in the green fluorescent protein and calmodulin-based fluorescent indicator constructs for Ca^{2+} called cameleons using steady-state and time-resolved spectroscopy of the full construct and of the component green fluorescent protein mutants, namely ECFP (donor) and EYFP (acceptor). EYFP displays a complicated photophysical behavior including protonated and deprotonated species involved in an excited-state proton transfer. When EYFP is excited in the absorption band of the protonated species, a fast nonradiative deactivation occurs involving almost 97% of the excited protonated population and leading to a low efficiency of excited-state proton transfer to the deprotonated species. ECFP displays a multiexponential fluorescence decay with a major contributing component of 3.2 ns. The time-resolved fluorescence data obtained upon excitation at 420 nm of Ca^{2+}-free and Ca^{2+}-bound YC3.1 cameleon constructs point to the existence of different conformations of calmodulin dependent on Ca^{2+} binding. Whereas steady-state data show only an increase in the efficiency of energy transfer upon Ca^{2+} binding, the time-resolved data demonstrate the existence of three distinct conformations/populations within the investigated sample. Although the mechanism of the interconversion between the different conformations and the extent of interconversion are still unclear, the time-resolved fluorescence data offer an estimation of the rate constants, of the efficiency of the energy transfer, and of the donor-acceptor distances in the Ca^{2+}-free and Ca^{2+}-bound YC3.1 samples.

INTRODUCTION

The green fluorescent protein (GFP) from the jellyfish *Aequorea victoria* and its mutants have been used extensively in molecular biology and cellular biology as genetically encoded markers (Chalfie, 1998; Sullivan and Kay, 1999; Tsien, 1998; Chalfie et al., 1994). Because their fluorescence occurs without the need of external cofactors and because they can be fused to other proteins in the ideal case without affecting their native functions, GFPs serve as a marker for gene expression, protein localization and many other cellular activities (Presley et al., 1997; Llopis et al., 1998; Hirose et al., 1999). The development of enhanced GFP variants with different emission colors made possible multicolor tracking of separate genes or fusion proteins and the creation of pairs of donors and acceptors for resonance energy transfer (Llopis et al., 2000; Vanderklish et al., 2000; Jensen et al., 2001). Because energy transfer occurs between two fluorophores in molecular proximity (less than 100 Å apart) and with overlap between fluorescence (donor) and absorption (acceptor) spectra, and because the efficiency of the energy transfer depends on the distance as well as orientation of the transition dipole moments of both donor and acceptor molecules, any signal that changes these two parameters will modulate the efficiency of the energy transfer (van der Meer et al., 1994). Hence, a donor-acceptor pair can be used as an in vivo reporter of different cellular activities or protein-protein interactions, depending on the linkage used to bring the two fluorophores in close proximity. Recently, Tsien et al. (Miyawaki et al., 1997, 1999) constructed genetically encoded fluorescent indicators for measuring Ca^{2+} signals in organelles by using pairs of GFP variants (either GFP blue or cyan mutants as donors and either EGFP or a modified EYFP mutant as acceptors (Miyawaki et al., 1999)), linked by calmodulin (CaM) and the calmodulin-binding peptide M13 (from myosin light chain kinase) and demonstrated their applicability as biochemical sensors. Binding of Ca^{2+} to the four binding sites of calmodulin results in wrapping of calmodulin around the M13 domain, resulting in the approach of the flanking proteins and hence to an increase in the efficiency of the energy transfer. Moreover, mutations performed on the calmodulin protein can tune Ca^{2+} affinities so that free Ca^{2+} concentrations in the 10^{-8} to 10^{-2} M range can be measured (Miyawaki et al., 1997). So far, cameleon proteins were used to estimate free Ca^{2+} concentration in cytosol, nucleus, and endoplasmic reticulum of individual cells (Miyawaki et al., 1997; Truong et al., 2001).

Because the concentration of Ca^{2+} is estimated from the efficiency of energy transfer, knowledge of the photophysical properties of both donor and acceptor fluorophores is required. Therefore, the photophysical properties of the two GFP variants used in the construction of the YC3.1 cameleon, i.e., ECFP (donor) and EYFP (acceptor), were investigated by means of ensemble time-correlated single photon counting

Submitted June 6, 2002, and accepted for publication August 1, 2002.

Satoshi Habuchi and Mircea Cotlet contributed equally to this work.

Address reprint requests to J. Hofkens, Department of Chemistry, Katholieke Universiteit Leuven, Celestijnenlaan 200F, 3001 Heverlee, Belgium. Tel.: +32-16-327804; Fax: +32-16-327990; E-mail: johan.hofkens@chem.kuleuven.ac.be.

0006-3495/02/12/3499/08 $2.00

spectroscopy. The same technique was used to reveal the dynamics and modifications of the efficiency of energy transfer between the two GFPs in the cameleon induced by the binding and dissociation kinetics of Ca^{2+}. Before this study, the wild-type GFP and several of its enhanced variants were the subject of intense photophysical studies, both at the ensemble (Striker et al., 1999; Cotlet et al., 2001a) and single molecule level (Dickson et al., 1997; Garcia-Parajo et al., 2000; Cotlet et al., 2001b), and as a result, a general and relatively complicated photophysical model accounting for the mechanism of the emission of GFPs was accepted (Lossau et al., 1996; Creemers et al., 1999; Winkler et al., 2002). It suggests excited state dynamics involving at least three forms of the chromophore and proton transfer (Chattoraj et al., 1996; Lossau et al., 1996). Depending on the mutant, this scheme might be even more complicated. With respect to the investigation of cameleons, Brasselet et al. (2000) studied at the single molecule level the dynamics and efficiency of FRET between ECFP and EYFP as partners in the YC2.1 cameleon for low, intermediate, and high Ca^{2+} concentration.

MATERIALS AND METHODS

Proteins and sample preparation

Enhanced cyan fluorescent protein (ECFP: F64L, S65T, Y66W, N146I, M153T, V63A, Clontech, Palo Alto, CA), enhanced yellow fluorescent protein (EYFP: S65G, V68L, S72A, T203Y, Clontech), and YC3.1 cameleon construct (linking ECFP, CaM, M13, and EYFP) were produced by standard recombinant techniques (Sambrook et al., 1989).

Spectroscopy

Ensemble steady-state and time-resolved spectroscopic measurements were performed at room temperature on 10^{-7} M sodium phosphate-buffered saline solutions of ECFP and EYFP (Sigma, St. Louis, MO), respectively, stored in 10-mm path length quartz cuvettes. For YC3.1, the cameleon construct was dissolved at 10^{-7} M concentration either in a Ca^{2+}-free or in a 0.1 mM Ca^{2+} containing sodium phosphate buffer (pH 7.4), resulting in Ca^{2+}-free and Ca^{2+}-bound YC3.1 samples that were finally stored in 10-mm path length quartz cuvettes. Based on the estimated dissociation constant of calcium binding to YC3.1 ($K_d = 1.5\ \mu$M according to Miyawaki et al., 1999), 90% of YC3.1 should bind to Ca^{2+} in the Ca^{2+}-bound YC3.1 sample.

Absorption spectra were measured using a spectrometer (Lambda 40, Perkin-Elmer, Wellesley, MA). Steady-state fluorescence excitation and emission spectra were measured using a spectrophotometer (Fluorolog 1500 Spex, Edison, NJ). The recorded fluorescence excitation and emission spectra were corrected according to literature procedures (Lakowicz, 1986). Time-resolved fluorescence measurements were performed using a time-correlated single photon counting method reported earlier (Cotlet et al., 2001a; Maus et al., 2001). Briefly, laser excitation was achieved by frequency doubling the output of a mode-locked picosecond Ti:Sapphire laser (Tsunami, 82-MHz repetition rate, Spectra Physics, Mountain View, CA) pumped by an Ar^+ laser (Beam Lok 2080, Spectra Physics) and then reducing the repetition rate to 8.13 MHz by an acousto-optical modulator (Pulse Selector 3980 Spectra Physics). Laser pulses were passed through a Berek polarization compensator (5540, New Focus, Santa Clara, CA) and a Glan polarizer to obtain vertically polarized excitation light at the sample. Fluorescence was collected in a right-angle geometry. Spectral separation was obtained with a stepper motor controlled subtractive double monochromator (Sciencetech 9030) and detected with a cooled micro-channel plate photomultiplier tube (E3059-500, Hamamatsu Photonics K.K., Hamamatsu, Japan). An additional polarizer was inserted in the emission path, oriented at magic angle (54.7°) with respect to the excitation polarization. The signal from the micro-channel plate photomultiplier tube was amplified in a fast rise time dual amplifier (8447 D, Hewlett-Packard, Palo Alto, CA) and input into a time-correlated single photon counting personal computer card (SPC630, Becker & Hickl GmbH, Berlin, Germany). Triggering was accomplished by sending 20% of the excitation laser beam to a nanosecond photodetector (818-BB-21, Newport, Irvine, CA). The experimental instrumental response function for all excitation wavelengths was in the 40- to 80-ps range. For each excitation wavelength, several decay curves at different emission wavelengths were collected in 4096 channels and with ~10,000 detected counts at the maximum of the fluorescence signal. Time-resolved emission spectra (TRES) using excitation at 420 nm, with a 5-nm step, were recorded from 450 up to 600 nm by time gating the single photon counting detection system and scanning the emission spectrum. Correction for the micro-channel plate photomultiplier tube spectral sensitivity was taken into account. Before and after each experiment, the sample was checked for photostability by recording the absorption spectrum. The time-resolved fluorescence decays were globally analyzed over the emission spectrum and for different time windows with a homemade program that uses a reweighted iterative reconvolution method based on the Marquardt algorithm. The contribution of the decay times recovered after the global analysis was estimated using the relative amplitudes:

$$a_j^{rel} = \frac{a_j \tau_j}{\sum_j a_j \tau_j} \quad (1)$$

The goodness of the fits was judged by the values of the reduced χ^2 as well as by inspecting the residuals for each fitted data set. The standard deviations of the fluorescence decay times were less than 20 ps for all decays. In the distance calculations for the cameleon protein, these standard deviations on the decay times will lead to an error of less than 1 Å. The main source of errors on the calculated distances is due to the value of orientation factor used (vide infra).

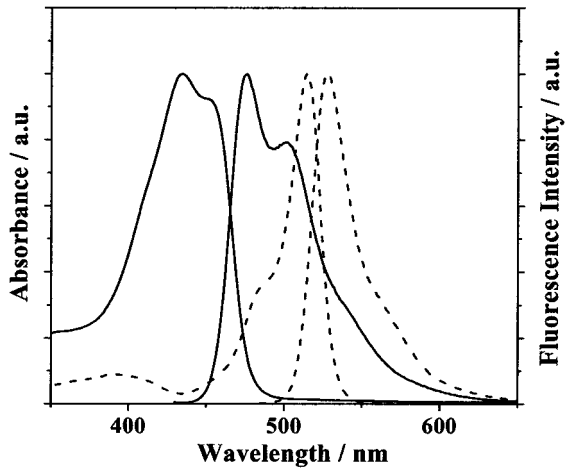

FIGURE 1 Absorption and emission spectra of phosphate-buffered saline solutions of EYFP (*dashed line*) and ECFP (*full line*). EYFP was excited at 488 nm while ECFP at 400 nm.

RESULTS AND DISCUSSION

Photophysics of the ECFP and EYFP variants

Fig. 1 shows the absorption and fluorescence spectra of the ECFP and EYFP dissolved in phosphate-buffered saline,

respectively. The absorption spectrum of EYFP displays a major peak at 514 nm attributed to the deprotonated form of the chromophore and a minor peak at 400 nm related to the protonated form, whereas fluorescence is emitted with a major peak at ~528 nm (Tsien, 1998). The extinction coefficient in the major peak was reported to be 83,400 M^{-1} cm^{-1} (Tsien, 1998), whereas the quantum yield of fluorescence (for excitation at 514 nm) was found as being 0.61 (Tsien, 1998). The red shifted emission of EYFP compared with the wild-type protein (from 504–528 nm) was explained by Tsien (1998). The fluorescence excitation spectrum of EYFP has a similar shape as the absorption spectrum, with a maximum at 514 nm, except for the band at ~400 nm, which is absent. The excitation spectrum detected at different emission wavelengths did not exhibit any spectral shift of the 514-nm peak as previously observed for EGFP (Cotlet et al., 2001a). Yellow fluorescence (λ_{max} = 528 nm) from EYFP was detected on excitation in both protonated and deprotonated absorption peaks with the same maximum at ~528 nm and no peak at lower wavelengths. However, excitation at 400 nm resulted in a decrease of the emitted fluorescence intensity compared with 514-nm excitation. These observations indicate the existence of a connection between the forms absorbing at 400 and 514 nm, respectively, probably via excited-state proton transfer (ESPT). However, the absence of the 400-nm peak from the excitation spectrum of EYFP would suggest a nonradiative deactivation of the protonated excited state competing with the ESPT. Indeed, the efficiency of the ESPT is estimated to be only 0.033 as calculated from the fluorescence quantum yield of EYFP excited at 400 nm (ϕ_f = 0.02) and 500 nm (ϕ_f = 0.61), respectively.

For ECFP, the substitution of Tyr with Trp in position 66 results in a new chromophore with an indole instead of a phenol or phenolate (Tsien, 1998). As a result, absorption and emission peaks occur at 435 and 450 nm (absorption) and 475 and 500 nm (emission). The absorption peaks have been previously ascribed to vibronic bands of the chromophore (Tsien, 1998). The extinction coefficient of ECFP at 435 was reported as being 32,500 M^{-1} cm^{-1} (Tsien, 1998). The fluorescence excitation and emission spectra of ECFP did not show excitation or detection wavelength dependencies.

Excitation of EYFP into the absorption band of the protonated form (400 nm) leads to a fast decay of the fluorescence when monitored at short wavelengths (between 440 and 480 nm). The fluorescence detected at 440 nm (Fig. 2 *A*) is built up by two decay time components of 6 and 60 ps with the short decay contributing to ~90% of the detected fluorescence. At longer wavelengths, i.e., 560-nm detection, the fluorescence decays monoexponentially with a time constant of 3.4 ns (Fig. 2 *B*). TRES recorded from 450 up to 600 nm upon 420-nm excitation are displayed in Fig. 3.

Following the time evolution of the emission spectrum, one can clearly see the presence, during the first 100 ps, of

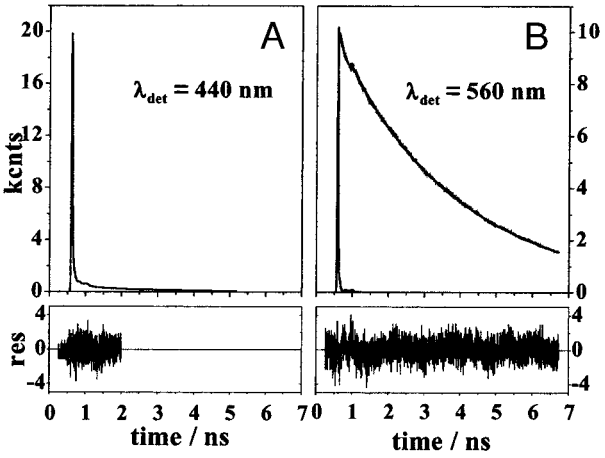

FIGURE 2 Fluorescence decays of EYFP excited at 400 nm and detected at 440 nm (*A*) and 560 nm (*B*).

the emission from the protonated form with a maximum at 480 nm. This band would account for the 6-ps decay component detected at 440 nm. The emission band related to the deprotonated form (peak at 528 nm) is present over the entire time window of the experiment. With respect to the fast components observed in the 440-nm decay, no corresponding rise time components were detected in the fluorescence decay monitored at 560-nm. Moreover, a deuterated solution of EYFP did not show any modification with respect to the recovered decay time components of both short (440 nm) and long (560 nm) wavelength detected fluorescence decays. Excitation of EYFP in the absorption band of the deprotonated form of the chromophore, either at 488 or 543 nm, led to a monoexponential decay of the detected fluorescence with a time constant of 3.4 ns. One

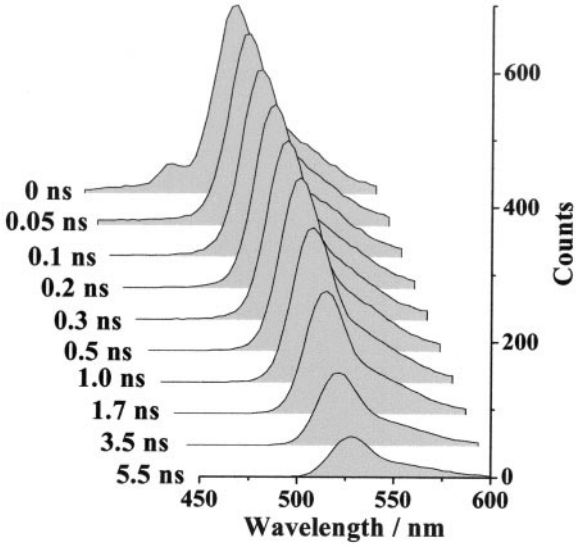

FIGURE 3 TRES of EYFP excited at 400 nm.

possible reason for the detected "yellow" fluorescence upon 400-nm excitation is the direct excitation of the deprotonated form, and another possibility for this fluorescence is due to ESPT. The efficiency of ESPT is estimated to be only 0.033 from the fluorescence quantum yield of EYFP excited at both 400 and 500 nm. This idea is supported also by the absence of the 400-nm peak from the excitation spectrum detected at 530 nm. Therefore, the contribution of the direct excitation of the deprotonated form to the "yellow" fluorescence may not be ignored even if the absorption of the deprotonated form at 400 nm is much smaller than that of the protonated form. Two different decay components of the fluorescence of the protonated form, 6 and 60 ps, would suggest, similarly as for EGFP, the existence of two subpopulations of the protonated chromophore for EYFP. Upon excitation at 400 nm, two corresponding excited-state protonated forms are created. One form, having a conformation that allows ESPT, relaxes to the deprotonated state within 60 ps while the other form decays radiatively to its corresponding ground state, and its fluorescence being quenched to 6 ps by a nonradiative process. The corresponding rise term for ESPT that should be seen in the emission band of the deprotonated form was not detected. The direct excitation of the deprotonated form would conceal the rise term in the decay detected at 560 nm. Fast internal conversion through rotational motion of the chromophore was recently suggested by Kummer et al. (1998, 2000) as the origin of the decay of fluorescence of the protonated form within few picoseconds in several variants carrying the T203Y mutation, such as the EYFP. In addition, femtosecond transient absorption spectroscopy has revealed that the decay of the protonated form is accompanied by rapid recovery of the ground state of the protonated form (averaged life time 0.006 ns) (Kummer et al., 2000). Moreover, the same group reported the detection of fast components in the time scale of tens of picoseconds showing decay and rise contributions at short- and long-detection wavelengths, respectively, for the variants carrying the T203Y mutation.

ECFP displays, independent of the detection wavelength, a multiexponential behavior for the detected fluorescence when excited at either 400 or 450 nm. The detected fluorescence is built up of three components of 0.24, 1.1, and 3.3 ns that contribute to the total fluorescence with 1%, 10%, and 89%, respectively. The TRES recorded upon excitation at 420 nm did not show any changes in position or shape compared with the corresponding steady-state fluorescence spectrum.

Although displaying a multiexponential fluorescence decay, indicating complicated photophysics, ECFP and EYFP still can be used to construct an energy transfer pair. The strong overlap of the emission spectrum of ECFP with the absorption spectrum of EYFP (Fig. 1), the relatively high quantum yield of fluorescence of ECFP (0.4), and the monoexponential decaying of fluorescence of EYFP when excited at the deprotonated band account for the use of this pair. Direct excitation of EYFP and hence "yellow" emission other than via energy transfer would not be a problem since from the total excited protonated population of EYFP only 3% would undergo ESPT. The multiexponential decay of ECFP, however, complicates the quantitation of the observed energy transfer between the two mutants.

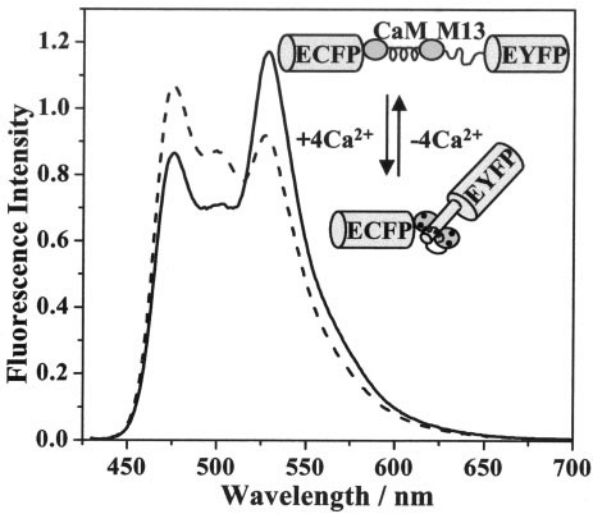

FIGURE 4 Steady-state fluorescence spectra of Ca^{2+}-free (*dotted line*) and Ca^{2+}-bound (*solid line*) YC3.1 excited at 420 nm.

Energy transfer dynamics in the YC3.1 cameleons

Fig. 4 shows the fluorescence spectra of Ca^{2+}-bound YC3.1 and Ca^{2+}-free YC3.1 detected upon 420-nm excitation. Because emission from EYFP at 528 nm is detected in the Ca^{2+}-free YC3.1 upon excitation of ECFP (Fig. 4), energy transfer occurs already in the absence of Ca^{2+}-binding to the YC3.1 calmodulin. Hence, already at this stage the acceptor (EYFP) is located within the Förster radius of the donor (ECFP). Ca^{2+}-binding to the calmodulin of YC3.1 results in an increase of the intensity of the 529-nm peak attributed to EYFP (Fig. 4) and hence an increase in the efficiency of the energy transfer. By estimating the efficiency of the energy transfer from the measured steady-state fluorescence spectra according to (van der Meer et al., 1994; Brasselet et al., 2000)

$$E = 1 - \frac{\phi_{DA}}{\phi_D} = \frac{(I_A/\phi_A)}{(I_A/\phi_A) + (I_D/\phi_D)} \qquad (2)$$

with I_D and I_A the integrated fluorescence intensities of the donor and of the acceptor, respectively, ϕ_D and ϕ_A the fluorescence quantum yields of the donor and acceptor, respectively, and ϕ_{DA} the fluorescence quantum yield of the donor in the presence of acceptor, values of the efficiency of the energy transfer 0.29 and 0.16 were found for the case of Ca^{2+}-bound and Ca^{2+}-free YC3.1, respectively. On the

other hand the efficiency of energy transfer is defined according to van der Meer et al. (1994) as

$$E = \frac{R_0^6}{R_0^6 + R^6} = \frac{k_{ET}}{k_{ET} + k_f} \quad (3)$$

$$R_0^6 = \frac{9000 \ln 10 \kappa^2 \phi}{128 \pi^5 n^4 N_A} \int \frac{f(\bar{V})\varepsilon(\bar{V})}{\bar{V}^4} d\nu \quad (4)$$

Here k_{ET} and k_f are the rate constants of energy transfer and fluorescence of donor in the absence of acceptor, respectively, R_0 and R are the critical transfer distance and the distance between the donor and the acceptor, respectively, κ^2 is orientation factor, ϕ is the fluorescence quantum yield of a donor, n is the refractive index of the solvent, N_A is Avogadro's number. The numerator from Eq. 4 refers to the overlap integral between the fluorescence emission of the donor and absorption of the acceptor. On the basis of the steady-state data measured for both GFP mutants and by assuming a random orientation of their transition dipole moments, R_0 was estimated to be 49 Å (Patterson et al., 2000). On the basis of the values for the efficiency of energy transfer estimated from the steady-state fluorescence data the distances between the donor (ECFP) and acceptor (EYFP) were estimated to be 65 Å for the Ca^{2+}-free YC3.1 and 57 Å for the Ca^{2+}-bound YC3.1. X-ray crystallographic (Ikura et al., 1992) and NMR experiments (Meador et al., 1992) show for the CaM-M13 complex in the Ca^{2+}-bound YC3.1 protein construct a compact globular shape, i.e., almost ellipsoidal with approximate dimensions of 47 by 32 by 30 Å. On the other hand, GFPs display a barrel-like shape having dimensions of 42-Å long and 24 Å in diameter and with the chromophore placed centrally on the symmetry axis of the barrel (Ormö et al., 1996; Yang et al., 1996). Therefore, the estimated R value for Ca^{2+}-bound YC3.1, i.e., 57 Å, is consistent with the proposed structure from Ikura et al. (1992) and Meador et al. (1992). In the absence of Ca^{2+}, calmodulin has a dumbbell-like structure with an overall length of 65 Å (Babu et al., 1988). In these conditions, taking into account the dimensions of GFP and M13, the distance between the GFP mutants in the protein construct in the case of Ca^{2+}-free YC3.1 should be larger than 120 Å if one assumes the most extended structure. The value of R_0 is calculated to be 66 Å, assuming perfectly oriented transition dipole moments, i.e., $\kappa^2 = 4$. Even for this condition, the efficiency of the energy transfer is estimated to be $E = 0.027$ if the protein adopts the most extended conformation ($R = 120$ Å). In the case of random orientation of the transition dipole moment, the energy transfer efficiency would be much smaller ($E = 0.0046$). For the Ca^{2+}-free YC3.1 sample, the estimated R value is 87 Å, assuming perfectly oriented transition dipole moments. This is the maximal R value that can be taken. Consequently, the steady-state data point to a relatively compact conformation of the protein construct, even in the Ca^{2+}-free condition. Such a conformation of the Ca^{2+}-free YC3.1 that allows energy transfer between the two GFP mutants points to the fact that calmodulin either does not adopt a stretched conformation in solution as in the crystal or interacts with M13-peptide even when Ca^{2+} does not bind to calmodulin.

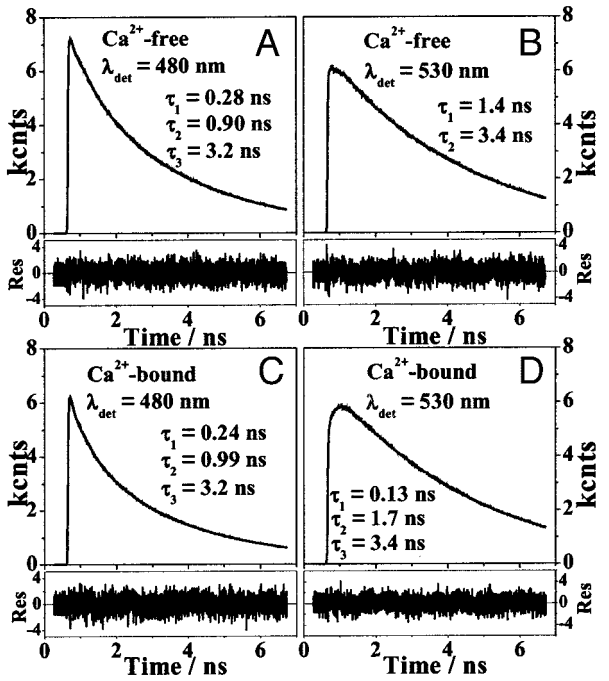

FIGURE 5 Fluorescence decays detected from Ca^{2+}-free YC3.1 and Ca^{2+}-bound YC3.1 samples upon excited at 420 nm. The detection wavelengths are indicated as insets. Fit and residual graphs are also depicted. Binding of Ca^{2+} to calmodulin results in the quenching of the 488-nm detected decays and delaying of the rise in the 530-nm detected decay as compared with the unbounded case.

Time-resolved fluorescence decays detected from both Ca^{2+}-bound and Ca^{2+}-free YC3.1 samples at the emission peak of either ECFP (480 nm) or EYFP (530 nm) upon 420-nm excitation display a complex multiexponential behavior (Fig. 5) including decay time components related to both GFP mutants and to energy transfer (vide infra).

For the Ca^{2+}-free YC3.1 sample, the decay detected at the emission peak of EYFP (Fig. 5 *B*) contains, apart from the 3.4-ns component reflecting the fluorescence decaying of EYFP, a supplementary component of 1.4 ns with negative contribution to the decay. For the Ca^{2+}-bound YC3.1 sample, the decay detected at the emission peak of EYFP (see Fig. 5 *D*) is built up mainly by the 3.4-ns component of EYFP and includes also two rise components of 0.13 and 1.7 ns. The decays detected at 480 nm for both Ca^{2+}-free and Ca^{2+}-bound samples are built up by three decay time components of 0.25, 1.0, and 3.3 ns. Similar decay components were found in the fluorescence decay of ECFP detected at 480 nm upon excitation at 420 nm. However, the contribution of the decay times differs for the three samples.

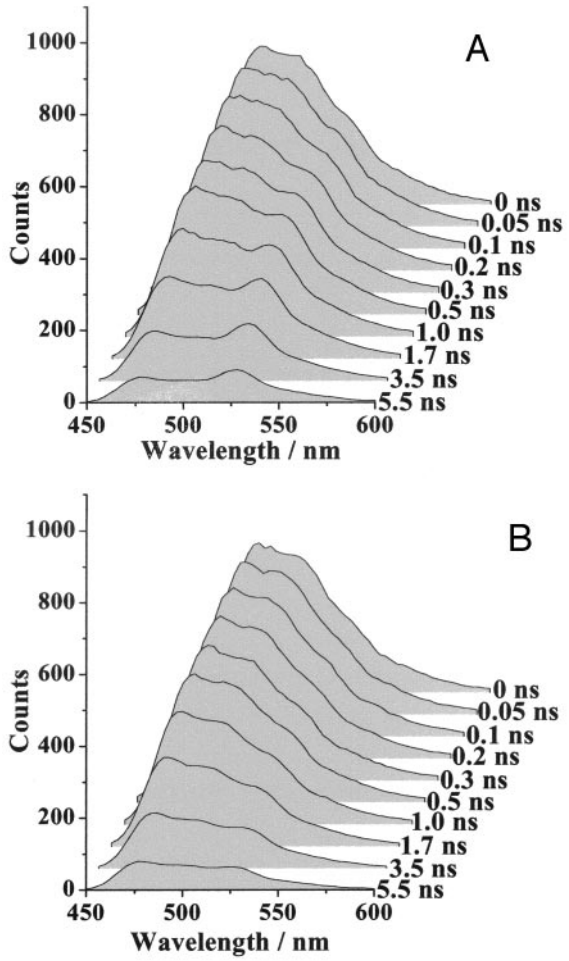

FIGURE 6 TRES of Ca^{2+}-bound (*A*) and Ca^{2+}-free (*B*) YC3.1 excited at 420 nm.

These observations suggest the existence of two regimes for energy transfer between the GFP mutants in the Ca^{2+}-bound YC3.1, i.e., slow (1.7 ns) and fast (0.13 ns) energy transfer and one regime for the case of Ca^{2+}-free YC3.1, a slow (1.4 ns) energy transfer. However, the presence in the short wavelength detected decays of unquenched fluorescence of ECFP for both Ca^{2+}-free and Ca^{2+}-bound samples points to the existence of a protein construct subpopulation that does not show energy transfer between the GFP mutants. Although the efficiency and rate constant of the energy transfer could not be obtained from the fluorescence decay of the donor molecule due to the complexity of the ECFP emission, we could get information on the energy transfer via the rise term of the acceptor molecule, EYFP (vide infra). An increasing of the efficiency of the process itself is clearly demonstrated by the steady-state fluorescence spectra (Fig. 4) and the TRES detected from the cameleons (Fig. 6, *A* and *B*).

Indeed, TRES detected upon excitation at 420 nm of Ca^{2+}-bound YC3.1 (Fig. 6 *A*) show, during their evolution over the probed time windows, a change in the intensity ratio between the 475- and 528-nm peaks related to emission from ECFP and EYFP, respectively, as compared with the case of Ca^{2+}-free YC3.1 (Fig. 6 *B*).

The time-resolved data presented here point to the existence of three regimes for energy transfer taking place between the two GFP mutants in the YC3.1 constructs, regimes that can be explained in terms of different conformations of the probed protein constructs and the equilibrium between the protonated and deprotonated form of the chromophore of EYFP. For both Ca^{2+}-free and Ca^{2+}-bound YC3.1 samples, part of the protein constructs would adopt a conformation such that energy transfer is blocked between the donor and acceptor. This points to a stretched conformation of calmodulin within the protein construct and might reflect the 10% YC3.1 that does not bind Ca^{2+} (see Materials and Methods). The equilibrium between the protonated and deprotonated form of EYFP would be another origin of the existence of a protein construct subpopulation that does not show energy transfer because the protonated chromophore of EYFP cannot act as an energy acceptor. It is calculated from the p*K*a of the EYFP chromophore (p*K*a = 7.0) and pH of the buffer (pH 7.4) that 28% of the EYFP is in the protonated form. The slow regime observed for both Ca^{2+}-free YC3.1 (1.4 ns) and Ca^{2+}-bound (1.7 ns) samples would account for a more compact conformation of the constructs for which the donor and acceptor approach to such a distance that energy transfer becomes possible. Since the rise components associated with energy transfer were evaluated by single decay analysis, and not with more reliable global analysis (Janssens et al., 1990), the 1.4- and 1.7-ns values might refer to the same conformation of the protein construct within both samples. Assuming a random orientation of transition dipole moments and an average decay time of 2.8 ns for the donor emitting alone on the basis of the recovered decay time components for ECFP, the 1.4- and 1.7-ns decay components related to energy transfer observed in Ca^{2+}-free YC3.1 and Ca^{2+}-bound YC3.1, respectively, would account (see Eq. 3) for an efficiency of 0.67 in the first case and 0.62 in the second case. According to Eq. 3, these efficiencies correspond to donor-acceptor distance of 44 and 45 Å for Ca^{2+}-free YC3.1 and Ca^{2+}-bound YC3.1, respectively. A construct that has these compact conformations will not act as a Ca^{2+} sensor because the conformation of the protein is uninfluenced by the binding/dissociation of Ca^{2+}. Upon Ca^{2+}-binding, the efficiency of energy transfer increases as found from the detected TRES and from the detection of an additional rise time of 0.13 ns for the Ca^{2+}-bound YC3.1 construct. Hence, the time resolved data presented here demonstrate that binding of Ca^{2+} leads to a folding of the protein construct that will favor energy transfer between ECFP and EYFP, similar to that previously discovered on the basis of x-ray crystallographic and NMR experiments (Ikura et al., 1992; Meador et al., 1992). Analogous calculations as for the case of slow en-

TABLE 1. Relative contribution of each conformation/population

Transfer efficiency	Protonated form $E = 0$	Extended form $E = 0$	Compact form $E = 0.62–0.67$	Folded form $E = 0.95$
Ca^{2+}-bound sample	28%	34%	23%	15%
Ca^{2+}-free sample	28%	47%	25%	

ergy transfer show for this situation an efficiency of 0.95 and hence accounts for a donor-acceptor distance of 30 Å.

The contribution of the different conformations/populations for both Ca^{2+}-free and Ca^{2+}-bound samples could be estimated by taking into account of the value of the energy transfer efficiency calculated on the basis of steady-state data and time-resolved data (Table 1).

The contribution of the extended form that does not undergo energy transfer is 34% and 47% for Ca^{2+}-bound and Ca^{2+}-free YC3.1, respectively. The contribution of the compact form ($E = 0.62–0.67$) that cannot be used as a Ca^{2+} sensor is almost constant for both conditions (23% and 25% for Ca^{2+}-bound and Ca^{2+}-free YC3.1, respectively). The contribution of the folded conformation ($E = 0.95$) that is observed only for Ca^{2+}-bound YC3.1 is 15%. In addition to these conformations, 28% of the protein construct cannot show energy transfer because it contains EYFP in the protonated state.

The existence of different conformations in YC2.1 cameleons was reported previously by Brasselet et al. (2000) on the basis of single molecule experiments. They pointed out an increase of the efficiency of energy transfer with the increasing of Ca^{2+} concentration and a broadening of the distribution of the energy transfer efficiency when Ca^{2+} concentration is set around the dissociation constant K_d for calmodulin. The observed broadening was related to a conformational dynamics of the cameleon construct due to the binding and dissociation kinetics of Ca^{2+}.

CONCLUSION

The photophysical properties of two GFP mutants, namely ECFP and EYFP, were investigated by means of steady-state and time-resolved spectroscopy to understand the dynamics of energy transfer in the YC3.1 cameleon containing these mutants as a donor-acceptor pair. EYFP displays a complicated photophysical behavior, similar to that found previously for EGFP, including protonated and deprotonated species involved in an ESPT. When EYFP is excited in the absorption band of the protonated species, a fast internal conversion involving almost 97% of the excited protonated population and leading to a low efficiency of ESPT to the deprotonated species and hence low emission of "yellow" fluorescence was observed. Upon excitation in the absorption band of the deprotonated chromophore, the monoexponential decaying of the detected "yellow fluorescence" indicates the emission from a single excited species. Combining this observation with the one related to the low efficiency of ESPT, the use of EYFP as an acceptor in a resonance energy transfer pair with ECFP is demonstrated. Upon excitation at either 420 or 450 nm, ECFP displays multiexponential decaying of fluorescence with a major contributing component of 3.3 ns, indicating possible emission from different species or the presence of different environments for the chromophore in ECFP.

The time-resolved fluorescence data obtained upon excitation at 420 nm of Ca^{2+}-free YC3.1 and Ca^{2+}-bound YC3.1 constructs point to the existence of different conformations of calmodulin with respect to the binding/dissociation of Ca^{2+} to calmodulin. Whereas steady-state data show only an increase of the efficiency of energy transfer upon Ca^{2+} binding, the time-resolved data demonstrate the existence of three distinct conformations/populations within the investigated sample offer an estimation of the rate constants, efficiency of the energy transfer, and the donor-acceptor distances in the investigated Ca^{2+}-free YC3.1 and Ca^{2+}-bound YC3.1 samples. It is also demonstrated that the presence of EYFP being in the protonated form has a large effect on the quantitative interpretation of the energy transfer data. In physiological conditions, the efficiency of the energy transfer will be significantly influenced by the small change of the pH since pKa of EYFP is 7.0. The presence of a subpopulation of the protein construct not undergoing energy transfer as found from time-resolved experiments, makes a quantitative estimation of the energy transfer within these protein constructs difficult and limits the use of the cameleons as sensitive Ca^{2+}-sensors. Furthermore, the exact enumeration of the populations is further complicated by eventual interconversions between the different conformations and by the possible photochemical modification of both donor and acceptor molecules.

The authors gratefully acknowledge the National Science Foundation (FWO) and the Flemish Ministry of Education for the support through GOA/1/2001, the support of the Federal Office for Scientific, Technological and Cultural Affairs (DWTC) through Grant IUAP-IV-11, and the support of the Katholieke Universiteit Leuven for an Interdisciplinair Onderzoeks (IDO) project. S.H. thanks the Japan Society for the Promotion of Science for a post-doctoral fellowship. The YC3.1 constructs were courtesy of the Tsien laboratory. We thank Dr. Thomas Gensch from Research Center Jülich for helpful discussions.

REFERENCES

Babu, Y. S., C. E. Bugg, and W. J. J. Cook. 1988. Structure of calmodulin refined at 2.2 Å resolution. *Mol. Biol.* 204:191–204.

Brasselet, S., E. J. G. Peterman, A. Miyawaki, and W. E. Moerner. 2000. Single-molecule fluorescence resonance energy transfer in calcium concentration dependent cameleon. *J. Phys. Chem. B.* 104:3676–3682.

Chalfie, M. 1998. Green Fluorescent Proteins, Properties, Applications and Protocols. Wiley-Liss, Inc, New York

Chalfie, M., Tu. G. Euskirchen, W. W. Ward, and D. C. Prasher. 1994. Green fluorescent protein as a marker for gene expression. *Science.* 263:802–805

Chattoraj, M., B. A. King, G. U. Bublitz, and S. G. Boxer. 1996. Ultra-fast excited state dynamics in green fluorescent protein: multiple states and proton transfer. *Proc. Natl. Acad. Sci. U. S. A.* 93:8362–8367.

Cotlet, M., J. Hofkens, F. Köhn, J. Michiels, G. Dirix, M. Van Guyse, J. Vanderleyden, and F. C. De Schryver. 2001b. Collective effects in individual oligomers of the red fluorescent coral protein DsRed. *Chem. Phys. Lett.* 336:415–423.

Cotlet, M., J. Hofkens, M. Maus, T. Gensch, M. Van der Auweraer, J. Michiels, G. Dirix, M. Van Guyse, J. Vanderleyden, A. J. W. G. Visser, and F. C. De Schryver. 2001a. Excited-state dynamics in the enhanced green fluorescent protein mutant probed by picosecond time-resolved single photon counting spectroscopy. *J. Phys. Chem. B.* 105:4999–5006.

Creemers, T. M. H., A. J. Lock, V. Subramaniam, T. M. Jovin, and S. Völker. 1999. Three photoconvertible forms of green fluorescent protein identified by spectral hole-burning. *Nat. Struct. Biol.* 6:557–560.

Dickson, R. M., A. B. Cubitt, R. Y. Tsien, and W. E. Moerner. 1997. On/off blinking and switching behavior of single molecules of green fluorescent protein. *Nature.* 388:355–358.

Garcia-Parajo, M. F., G. M. J. Segers-Nolten, J.-A. Veerman, J. Greve, and N. F. van Hulst, 2000. Real-time light-driven dynamics of the fluorescence emission in single green fluorescent protein molecules. *Proc. Natl. Acad. Sci. U. S. A.* 97:7237–7242.

Hirose, K., S. Kadowaki, M. Tanabe, H. Takeshima, and M. Iino. 1999. Spatiotemporal dynamics of inositol 1,4,5-triphosphate that underlies complex Ca^{2+} mobilization patterns. *Science.* 284:1527–1530.

Ikura, M., G. M. Clore, A. M. Gronenborn, G. Zhu, C. B. Klee, and A. Bax. 1992. Solution structure of a calmodulin-target peptide complex by multidimensional NMR. *Science.* 256:632–638.

Janssens, L. D., N. Boens, M. Ameloot, and F. C. De Schryver. 1990. A systematic study of the global analysis of multiexponential fluorescence decay surfaces using reference convolution. *J. Phys. Chem.* 94: 3564–3576.

Jensen, K. K., L. Martini, and T. W. Schwartz, 2001. Enhanced fluorescence resonance energy transfer between spectral variants of green fluorescent protein through zinc-site engineering. *Biochemistry.* 40: 938–945.

Kummer, A. D., C. Kompa, H. Lossau, F. Pollinger-Dammer, M. E. Michel-Beyerle, C. M. Silva, E. Bylina, W. J. Coleman, M. M. Yang, and D. C. Youvan. 1998. Dramatic reduction in fluorescence quantum yield in mutants of green fluorescent protein due to fast internal conversion. *Chem. Phys.* 237:183–193.

Kummer, A. D., J. Wiehler, H. Rehaber, C. Kompa, B. Steipe, and M. E. Michel-Beyerle. 2000. Effects of threonine 203 replacements on excited-state dynamics and fluorescence properties of the green fluorescent protein (GFP). *J. Phys. Chem. B.* 104:4791–4798.

Lakowicz, J. R. 1986. Principles of Fluorescence Spectroscopy. Plenum Press, New York.

Llopis, J., J. M. McCaffery, A. Miyawaki, M. G. Farquhar, and R. Y. Tsien. 1998. Measurement of cytosolic, mitochondrial, and golgi pH in single living cells with green fluorescent proteins. *Proc. Natl. Acad. Sci. U. S. A.* 95:6803–6808.

Llopis, J., S. Westin, M. Ricote, J. Wang, C. Y. Cho, R. Kurokawa, T.-M. Mullen, D. W. Rose, M. G. Rosenfeld, R. Y. Tsien, and C. K. Glass, 2000. Ligand-dependent interactions of coactivators steroid receptor coactivator-1 and peroxisome proliferator-activated receptor binding protein with nuclear hormone receptors can be imaged in live cells and are required for transcription. *Proc. Natl. Acad. Sci. U. S. A.* 97: 4363–4368.

Lossau, H., A. Kummer, R. Heinecke, F. Pöllinger-Dammer, C. Kompa, G. Bieser, T. Jonsson, C. M. Silva, M. M. Yang, D. C. Youvan, and M. E. Michel-Beyerle. 1996. Time-resolved spectroscopy of wild-type and mutant green fluorescent proteins reveals excited state deprotonation consistent with fluorophore-protein interactions. *Chem. Phys.* 213:1–16.

Maus, M., E. Rousseau, M. Cotlet, J. Hofkens, G. Schweitzer, M. Van der Auweraer, F. C. De Schryver, and A. Kruegen, 2001. New picosecond laser system for easy tunability over the whole ultraviolet/visible/near infrared wavelength range based on flexible harmonic generation and optical parametric oscillation. *Rev. Sci. Instrum.* 72:36–40.

Meador, W. E., A. R. Means, and F. A. Quiocho. 1992. Target enzyme recognition by calmodulin: 2.4 Å structure of a calmodulin-peptide complex. *Science.* 257:1251–1254.

Miyawaki, A., O. Griesbeck, R. Heim, and R. Y. Tsien. 1999. Dynamic and quantitative Ca^{2+} measurements using improved cameleons. *Proc. Natl. Acad. Sci. U. S. A.* 96:2135–2140.

Miyawaki, A., J. Llopis, R. Heim, J. M. McCaffery, J. A. Adams, M. Ikura, and R. Y. Tsien. 1997. Fluorescent indicators for Ca^{2+} based on green fluorescent proteins and calmodulin. *Nature.* 388:882–887.

Ormö, M., A. B. Cubitt, K. Kallio, L. A. Gross, R. Y. Tsien, and S. J. Remington. 1996. Crystal structure of the *aequorea victoria* green fluorescent protein. *Science.* 273:1392–1395.

Patterson, G. H., D. W. Piston, and B. G. Barisas, 2000. Förster distances between green fluorescent protein pairs. *Anal. Biochem.* 284:438–440.

Presley, J. F., N. B. Cole, T. A. Schroer, K. Hirschberg, K. J. M. Zaal, and J. Lippincott-Schwartz, 1997. ER-to-golgi transport visualized in living cells. *Nature.* 389:81–85.

Sambrook, J., E. F. Fritsch, and T. Maniatis. 1989. Molecular Cloning: A Laboratory Manual, 2nd ed. Cold Spring Harbor Laboratory Press, Cold Spring Harbor, NY.

Striker, G., V. Subramaniam, C. A. M. Seidel, and A. J. Volkmer. 1999. Photochromicity and fluorescence lifetimes of green fluorescent protein. *J. Phys. Chem. B.* 103:8612–8617.

Sullivan, K. F., and S. A. Kay. 1999. Green Fluorescent Protein. Academic Press, San Diego, CA.

Truong, K., A. Sawano, H. Mizuno, H. Hama, K. I. Tong, T. K. Mal, A. Miyawaki, and M. Ikura, 2001. FRET-based in vivo Ca^{2+} imaging by a new calmodulin-GFP fusion molecule. *Nat. Struct. Biol.* 8:1069–1073.

Tsien, R. Y. 1998. The green fluorescent protein. *Annu. Rev. Biochem.* 67:509–544.

Vanderklish, P. W., L. A. Krushel, B. H. Holst, J. A. Gally, and K. L. Crossin, 2000. Marking synaptic activity in dendritic spines with a calpain substrate exhibiting fluorescence resonance energy transfer. *Proc. Natl. Acad. Sci. U. S. A.* 97:2253–2258.

Vander Meer, B. W., G. Coker, and S.-Y. S. Chen. 1994. Resonance Energy Transfer: Theory and Data. VCH Publisher, New York.

Winkler, K., J. R. Lindner, V. Subramaniam, T. M. Jovin, and P. Vohriger, 2002. Ultrafast dynamics in the excited state of green fluorescent protein (wt) studied by frequency-resolved femtosecond pump-probe spectroscopy. *Phys. Chem. Chem. Phys.* 4:1072–1081.

Yang, F., L. G. Moss, and G. N. Phillips. 1996. The molecular structure of green fluorescent protein. *Nat. Biotech.* 14:1246–1251.